International Journal of Nanomedicine

Dovepress
open access to scientific and medical research

Open Access Full Text Article

ORIGINAL RESEARCH

Novel Carbon Dots Derived from *Moutan Cortex* Significantly Improve the Solubility and Bioavailability of Mangiferin

Chuihao Kong[1,2,*], Kaidi Wang[1,2,*], Lei Sun[1,3], Hongsu Zhao[1,2], Tongsheng Wang[1], Wuxi Zhou[1], Deling Wu[1,2], Fengqing Xu[1,2]

[1]School of Pharmacy, Anhui University of Chinese Medicine, Hefei, 230012, People's Republic of China; [2]Anhui Province Key Laboratory of New Manufacturing Technology for Traditional Chinese Medicine Decoction Pieces, Hefei, 230012, People's Republic of China; [3]Zhejiang CONBA Pharmaceutical Co. LTD, Hangzhou, 310052, People's Republic of China

*These authors contributed equally to this work

Correspondence: Wuxi Zhou; Fengqing Xu, School of Pharmacy, Anhui University of Chinese Medicine, 350 Longzihu Road, Xinzhan District, Hefei, 230012, People's Republic of China, Email zhouwuxi@ahtcm.edu.cn; xufengqing@ahtcm.edu.cn

Background: Mangiferin (MA), a bioactive C-glucosyl xanthone with a wide range of interesting therapeutic properties, has recently attracted considerable attention. However, its application in biomedicine is limited by poor solubility and bioavailability. Carbon dots (CDs), novel nanomaterials, have immense promise as carriers for improving the biopharmaceutical properties of active components because of their outstanding characteristics.

Methods: In this study, a novel water-soluble carbon dot (MC-CDs) was prepared for the first time from an aqueous extract of *Moutan Cortex Carbonisata*, and characterized by various spectroscopies, zeta potential and high-resolution transmission electron microscopy (HRTEM). The toxicity effect was investigated using the CCK-8 assay in vitro. In addition, the potential of MC-CDs as carriers for improving the pharmacokinetic parameters was evaluated in vivo.

Results: The results indicated that MC-CDs with a uniform spherical particle size of 1–5 nm were successfully prepared, which significantly increased the solubility of MA in water. The MC-CDs exhibited low toxicity in HT-22 cells. Most importantly, the MC-CDs effectively affected the pharmacokinetic parameters of MA in normal rats. UPLC-MS analysis indicated that the area under the maximum blood concentration of MA from mangiferin-MC-CDs (MA-MC-CDs) was 1.6-fold higher than that from the MA suspension liquid (MA control) after oral administration at a dose of 20 mg/kg.

Conclusion: *Moutan Cortex*-derived novel CDs exhibited superior performance in improving the solubility and bioavailability of MA. This study not only opens new possibilities for the future clinical application of MA but also provides evidence for the development of green biological carbon dots as a drug delivery system to improve the biopharmaceutical properties of insoluble drugs.

Keywords: *Moutan Cortex*, carbon dots, mangiferin, solubility, bioavailability

Introduction

Mangiferin (MA), a natural *C*-glucosyl xanthone scaffold initially isolated from *Mangifera indica*, exhibits a wide range of interesting pharmacological activities, such as cardioprotective, immunomodulatory, antioxidant, antitumor, antidiabetic, and anti-inflammatory effects.[1–7] The therapeutic significance of MA has made it attractive for the research and development of drugs and food supplements over decades. Nonetheless, some limitations caused by the structural type of xanthone *C*-glycoside, including scarce solubility in water and low bioavailability, severely restrict its clinical applications.[8] Currently, several studies on solubilization methods have been conducted to improve the water solubility and bioavailability of MA, but there is still a lack of satisfactory outcome.[9–16] Therefore, developing new materials and

Received: 23 January 2024
Accepted: 14 April 2024
Published: 20 April 2024

Graphical Abstract

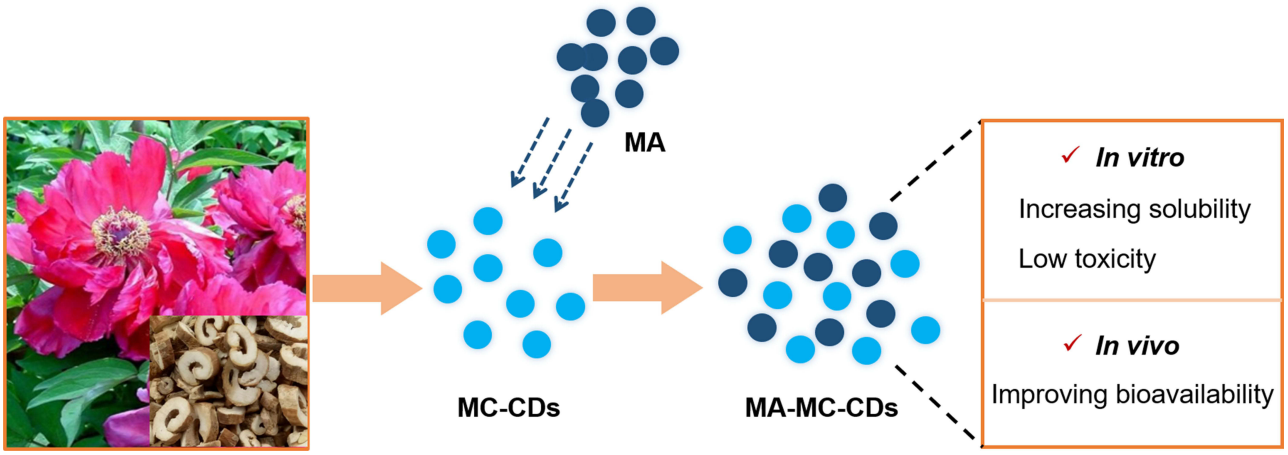

techniques to improve MA's biopharmaceutical properties of MA is a challenging issue and requires a considerable amount of effort.

The hydrophilicity and bioavailability of insoluble active components can be improved by making into nanomaterials which are a special class of materials with unique physical, chemical, and biological properties.[17–20] Many studies have aimed at developing novel nanomaterial-based sensors for applications in biology and medicine, while their clinical applications are greatly restricted by high cost and adding highly toxic components.[21–23] As novel nanomaterials, carbon dots (CDs) have gained particular attention in recent years owing to their outstanding characteristics and wide-ranging pharmaceutical applications.[24–38] In particular, their small size and large surface area make them highly water-soluble and biocompatible, which holds great promise for drug delivery. However, most CDs are chemically synthesized derivatives using multiple materials which biocompatibility and biological security falls short of that of natural sources.[39–41] *Moutan Cortex* (MC), a well-known Traditional Chinese Medicine, has a long history of medical applications in China and other Asian countries. Modern studies have shown that MC has antioxidant, anti-cancer, hypoglycemic, anti-aggregatory, anti-inflammatory, and antiallergic properties, and other effects.[42–46] The structures in MC make it advantageous for the formation of nanoclusters.[47] Recently, we made an interesting discovered that a novel carbon dot (MC-CDs) derived from MC, the only source, exhibited significant potential for applications in biology and medicine, and further proposed the hypothesis that MC-CDs can serve as a natural carrier, holding potential for improving the solubility and bioavailability of MA.

In this study, for the first time, we evaluated the *Moutan Cortex*-carbon dots in particle size, structural details, fluorescence behavior, elemental composition, and surface functional groups. The biopharmaceutical properties were investigated in vivo and in vitro and showed superior performance in terms of improving the solubility and bioavailability of MA. This study not only opens new possibilities for the future clinical application of MA but also provides evidence for the development of green biological carbon dots as a drug delivery system to improve the biopharmaceutical properties of insoluble drugs.

Materials and Methods

Materials and Chemicals

The root bark of *Paeonia ostii* was collected from Anhui Tongling Hetian Traditional Chinese Medicine Pieces Co., Ltd. and identified by associate-Prof. QingShan Yang, Anhui University of Traditional Chinese Medicine. MC-CDs were prepared in our laboratory. MA and isomangiferin with a purity > 98.0% were provided by Wuhan ChemFace

Biotechnology Co., Ltd., and a dialysis bag with a molecular mass of 3000 Da was purchased from Sigma-Aldrich St. Louis. All chemical reagents were of chromatographic or analytical grade.

Animals

Male Sprague-Dawley rats (weighing 200 ± 20 g) were obtained from Animal Certificate No. SCXK (Lu) 2019–0003 was purchased from Jinan Pengyue Experimental Animal Breeding Co., Ltd. (Jinan, China). After 1 week of feeding, the animal experiments were performed according to the animal protocol of the Animal Ethics Association of Anhui University of Chinese Medicine (Ethics number: AHUCM-rats-2022104).

Preparation of MC-CDs

Carbonized *Moutan Cortex* was obtained by pyrolysis method (Figure 1). Briefly, an open crucible containing the dry root bark of *P. ostii* was wrapped in aluminum foil, sealed with a lid, and placed in a muffle furnace (KSL-1700X, Hefei Kejing Material Technology Co., Ltd.). The carbonized *Moutan Cortex* was obtained according to the following procedure: the temperature was raised to 350°C within an hour, insulated for 1 h, and then cooled to room temperature. The carbonized product was crushed into powder, placed in a beaker, and extracted three times with deionized water (10 times, 2 h each) at 100°C. The filtrate was concentrated using a rotary evaporator, and the concentrated liquid was centrifuged at 5000 rpm for 10 min to remove the insoluble material and then loaded into the treated 3000 Da dialysis bag. The water was changed after some time, and dialysis was carried out for 4 days. The dialysis inner liquid was freeze-dried to obtain *Moutan Cortex*-Carbon dots (MC-CDs).

Characterization Study of MC-CDs

TEM analysis was performed using a Talos F200X electron microscope (Thermo Fisher Scientific). HRTEM was performed using a JEM-2100 Transmission electron microscope (JEOL, Japan) to determine the dispersion and morphology of CDs. IR spectra were obtained on a Nicolet 6700 FT-IR spectrometer (Thermo Fisher Scientific, USA) with KBr pellets in the range–4000-1000 cm^{-1}. Absorption and fluorescence measurements were performed using a UV-visible spectrophotometer (Specord S600, Analytik JENA, Germany) and F-450 fluorescence spectrophotometer (Toyko, Japan). The determination of the atoms contained in the carbon quantum dots of MC and their percentage contents were verified via X-ray photoelectron spectroscopy (XPS, ESCALAB 250, Thermo Fisher Scientific), X-ray diffraction (XRD) was performed with X-ray diffractometer (SmartLab). Zeta potential was carried out on Zetasizer Nano ZS (Malvern Panalytical Ltd.). All statistical graphs were made in Origin 2021 software.

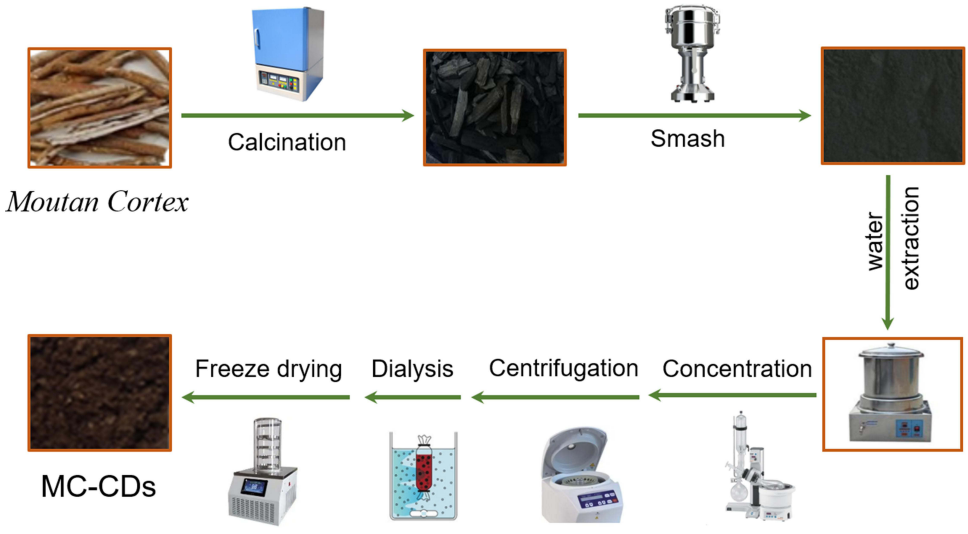

Figure 1 Preparation scheme of *Moutan Cortex*-Carbon dots (MC-CDs).

Measurement of Fluorescence Quantum Yields

Fluorescence quantum yield was acquired according to a method described as reported.[17] Briefly, Quinine sulfate was used as the control standard (quantum yield 54% in 0.1 M sulfuric acid solution). The absorbance of the aqueous solution of the MC-CDs and control sample was maintained below 0.10 at 350 nm. The fluorescence yield was determined by integrating the established procedure. The fluorescence quantum yield was calculated using the following equation:

$$\theta_t = \theta_{c\times} \frac{A_t}{I_c} \times \frac{I_t}{A_c} \times \frac{(\eta_t)^2}{(\eta_c)^2}$$

where "θ" is the fluorescence quantum yield, "A" is the absorbance at the excitation wavelength (350 nm), and "I" is the refractive index of the solvent, the subscripts "t" and "c" refer to the test (MC-CDs) and the standard (quinine sulfate), respectively.

Cytotoxicity Assays

HT-22 cells were cultured at 37°C in 5% CO_2 in Dulbecco's modified Eagle's medium (DMEM; Gibco Inc., NY, USA) supplemented with 100 U/mL penicillin, 100 μg/mL streptomycin, and 10% fetal bovine serum (FBS; Gibco Inc., NY, USA). The MC-CDs were dissolved in deionized water and diluted with the cell culture medium to obtain the desired concentrations. The cells were seeded into 96-well plates at a density of 1×10^5 cells/well and incubated with 10% fetal bovine serum medium and different concentrations of MC-CDs. After incubation for 24 h, cell survival was determined using the CCK-8 method.[48]

Water Solubility Assay

First, MA (3.2 mg) and isomangiferin (3.0 mg) were placed in 10 mL volumetric flasks, dissolved in ultrapure water, sonicated, and centrifuged to prepare saturated aqueous solutions of standards. The saturated solution was transferred and diluted 10-, 50-, 100, and 500 times to get the corresponding sample solutions to measure their water solubility. Subsequently, the concentration of MC-CDs (30 mg dissolved in 10 mL aqueous solution) was diluted to 10 grades in the concentration range of 1500 to 3.12 μg/mL. Next, in a 5 mL EP tube, 2 mg of MA or isomangiferin was accurately weighed, and then 1mL corresponding concentration of the MC-CDs solution was added, which resulted in a mixed saturated solution after sonication in an ultrasonic cleaner at 480 W for 30 min. The obtained solution was centrifuged at 10000 rpm for 10 min, and the supernatant was collected and filtered through a 0.22 μm membrane prior to injection. Chromatographic analyses of all the standards and samples were performed a Shimadzu 2030 C HPLC instrument (Shimadzu, Japan). Chromatographic separation was carried out at 30°C on a Phenomenex-C18 column (250 mm ×4.6 mm, 5 μm, USA), and eluted with 0.4% glacial acetic acid water (A)-acetonitrile (B) = 85:15, at 1.0 mL/min. Every 20 μL solution was injected for each run, and the PDA spectra were recorded at 318 nm. Calibration curves and methodological investigation experiments were performed according to the methods of the Chinese Pharmacopoeia.[49]

Pharmacokinetic Experiments

MA was added to an aqueous solution of MC-CDs and stirred for 20 min to obtain a saturated suspension of mangiferin-MC-CDs (MA-MC-CDs). MA was dissolved in an aqueous solution to obtain an MA suspension liquid (MA control). Rats were fasted, but provided free drinking 12 h prior to drug administration. MA-MC-CDs (2 mg/mL) and the MA control (2 mg/mL) were administered via oral gavage at a dose of 20 mg/kg. 0.5 mL blood was collected from the orbit at each time point of 5 min, 15 min, 30 min, 45 min, 60 min, 120 min, 240 min, 480 min, 720 min, 1440 min. Blood was placed in an EP tube containing heparin sodium, centrifuged at 4000 rpm for 5 min, and plasma was obtained.

A 400 μL mixture solution of acetonitrile and glacial acetic acid at a ratio of 9:1 (v:v) was added to 100 μL plasma, vortexed, and centrifuged at 10000 rpm for 10 min, and the supernatant was collected and evaporated using liquid nitrogen to obtain the dry residue. The residue and the internal standard (isomangiferin) were dissolved in the mobile phase and centrifuged at 10,000 rpm for 10 min. The obtained supernatant was analyzed using a SCIEX TRIPLE QUAD 4500 Triple Quadrupole Series Mass Spectrometer (UHPLC-QTRAP-MS/MS, AB SCIEX, USA).

Chromatographic separation was carried out at 30°C on a ACQUITY UPLC BEH C18 column (2.1 mm × 100 mm × 1.7 μm), and eluted with 0.4% glacial acetic acid water (A)-acetonitrile (B) = 90:10, at 0.2 mL/min. Every 3 μL of the solution was injected for each run, and the total ion chromatogram (TIC) was recorded at DP: −38V and CE: −32V.

Statistical Analysis

The data were presented as mean ± S.D. All values were analyzed using a one-way analysis of variance (ANOVA) and LSD-*t* test by IBM SPSS Statistics 23.0, The statistical graphs were generated using Graph-Pad Prism 8.0 software and Origin 2021. P values < 0.05 were considered statistically significant.

Results

Characteristics of MC-CDs

The TEM image of the MC-CDs (Figure 2A) revealed that they were nearly spherical with a size distribution in the range of 1–5 nm (Figure 2B). Furthermore, the HRTEM (Figure 2C) showed that the CDs have a lattice spacing of 0.10 nm (Figure 2D). The UV-vis spectrum (Figure 2E) of the aqueous MC-CDs solution exhibited a broad absorption spectrum at 200–300 nm. The photoluminescence spectra of the MC-CDs in aqueous solutions exhibited the strongest emission at approximately 445 nm, with the strongest excitation at 350 nm. XRD analysis confirmed the amorphous nature of prepared MC-CDs. A broad peak at 2θ = 22.1° was exhibited in the XRD pattern of MC-CDs (Figure 2G), indicating the presence of crystal planes of graphitic carbon (002)[50,51] in MC-CDs. In addition, some weak peaks can be observed. The crystal plane 110 at 2θ = 37.1° showed that MC-CDs possessed monolayer crystal structure. The crystal plane 101 at 2θ = 45.3° indicated that MC-CDs have hexagonal structure. We then measured the zeta potential of MC-CDs and found that the value was negative charge −25.20 mV (Figure 2H), demonstrating its stability and biocompatible.[52]

To gain a better insight into the organic functional groups on the surface of the MC-CDs, we further analyzed the MC-CDs using FTIR (Figure 2F). The peaks in the IR spectra were assigned according to the Sadtler Handbook of Infrared Spectra. The character absorption bands at 3548, 3474 cm^{-1} ascribable to hydroxyl groups, and 3410, 3236 cm^{-1} represent stretching vibrations of amino groups (N-H); The typical stretching vibrations of C=O and C=C could be observed at 1776, 1639 and 1618 cm^{-1}; The peak located at 1385 cm^{-1} can be attributed to stretching vibrations of ester groups, and the peak at 1137 cm^{-1} was due to the asymmetric and symmetric stretching vibrations of C-O or C-N groups.

The surface chemical properties and characteristics of the MC-CD functional groups were determined using XPS. As shown in Figure 3A, the three peaks of the full-survey XPS at 285.0, 400.0 and 533.0 eV correspond to C1s, O1s, and N1s, respectively. This spectral result exhibited that the MC-CDs are composed of carbon, oxygen, and nitrogen with atomic percentages of 63.38%, 34.47% and 2.16%, respectively. In the high-resolution C1s spectrum, three different peaks correspond to carbon for C-C/C=C (284.8 eV), C-O (286.4 eV), and O-C=O (288.5 eV) (Figure 3B). The high-resolution O1s spectrum indicated different chemical environments of C=O (531.8 eV), and C-O (532.9 eV) (Figure 3C). Moreover, the peaks in the high-resolution scans of the N1s region correspond to nitrogen for C-N at 399.9 eV, and N-$(C)_3$ at 401.1 eV (Figure 3D).

To further characterize the products, the luminescence properties of MC-CDs were evaluated. The fluorescence emission spectrum of the prepared MC-CDs exhibited the strongest peak at 440 nm upon excitation at 340 nm (Figure 4A). Figure 4B shows the excitation spectra of MC-CDs at emission wavelengths progressively increasing from 300 to 340 nm and decreasing from 360 to 460 nm. Figure 4C shows the emission spectra of MC-CDs at excitation wavelengths progressively increasing from 400 to 440 nm and decreasing from 460 to 560 nm.

Cytotoxicity Evaluation of MC-CDs

To investigate the safety of the MC-CDs, their cytotoxicity was evaluated in HT-22 cells. As shown in Figure 5, even when the concentration of MC-CDs reached up to 640 μg/mL, the cell viability was still greater than 90%, even when the concentration of MC-CDs reached 640 μg/mL. MC-CDs significantly increased the viability of MDA-MB-231 cells in a dose-dependent manner (1.25–80 μg/mL), indicating that MC-CDs promoted cell growth. These results indicate that MC-CDs could be bio-safe in normal cells.

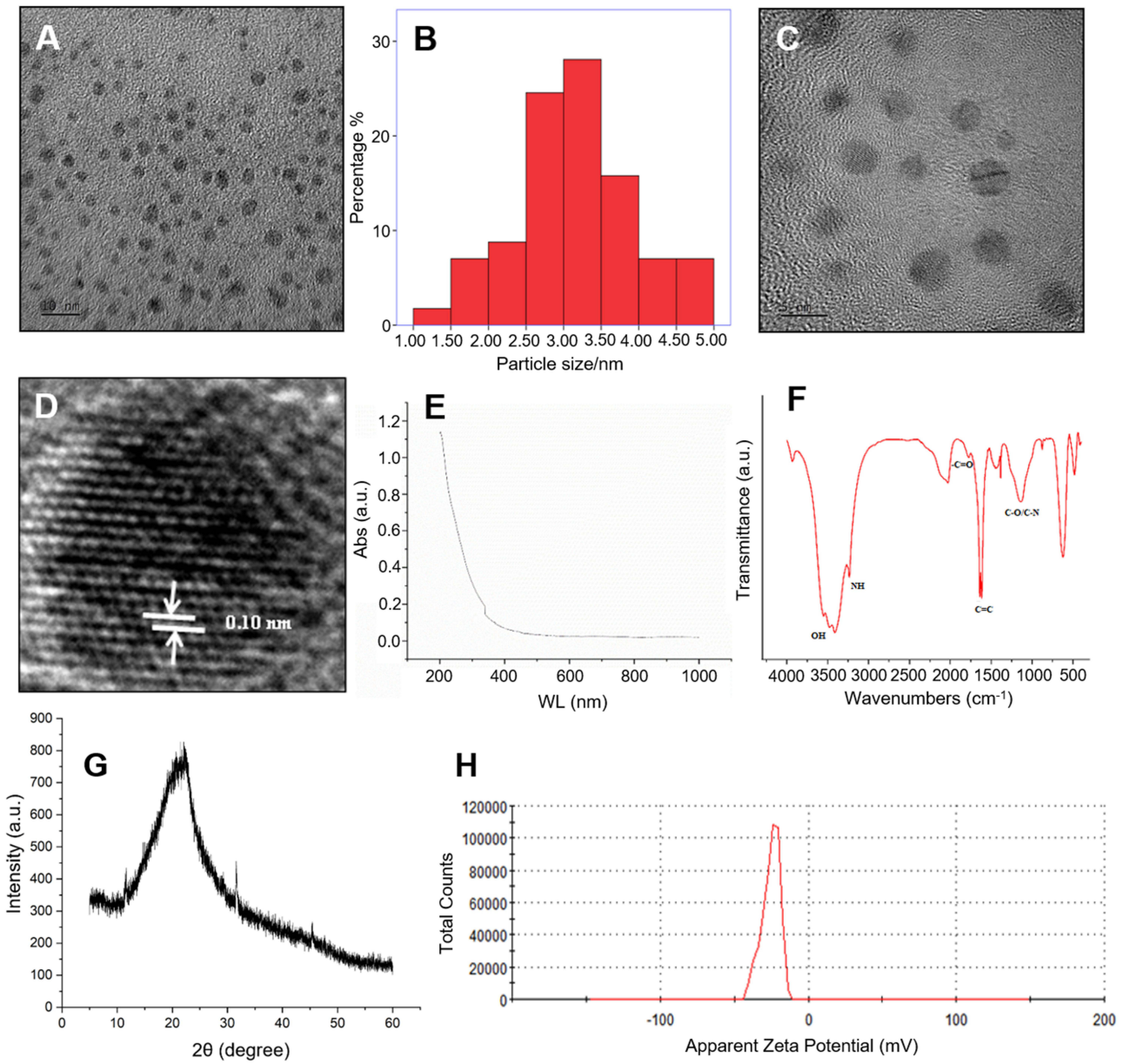

Figure 2 Characteristics of MC-CDs. (**A**) Transmission Electron Microscope (TEM) of MC-CDs. (**B**) TEM size distribution of MC-CDs. (**C**) High Resolution Transmission Electron Microscope of MC-CDs. (**D**) Lattice spacing of MC-CDs in HRTEM. (**E**) Ultraviolet-visible spectroscopy (UV-Vis) of MC-CDs. (**F**) Fourier-transform infrared spectrometer (FTIR) of MC-CDs. (**G**) XRD pattern of MC-CDs. (**H**) Zeta potential values of MC-CDs.

Solubility Study

In this study, an HPLC method was established and validated for the determination of MA in an MC-CDs aqueous solution. The solubility of MA in water was 115.46 μg/mL, and the linear equation was y = 21,863.4253x-17,396.5833 r = 1.0000. As shown in Figure 6, the concentration of MA increased with increasing concentrations of MC-CDs. The RSD values of the peak area and retention time of the samples were calculated methodologically; the RSD value of the peak area of the precision was 0.09%, the RSD value of the retention time was 0.22%, the RSD value of the stability peak area was 1.10%, the RSD value of the retention time was 1.31%, the reproducible peak area RSD value was 2.92%, the retention time RSD value was 2.49%, and the recovery rate of the sample was 100.68%~102.78%; It shows that the proposed method was good and the prepared samples were relatively stable.

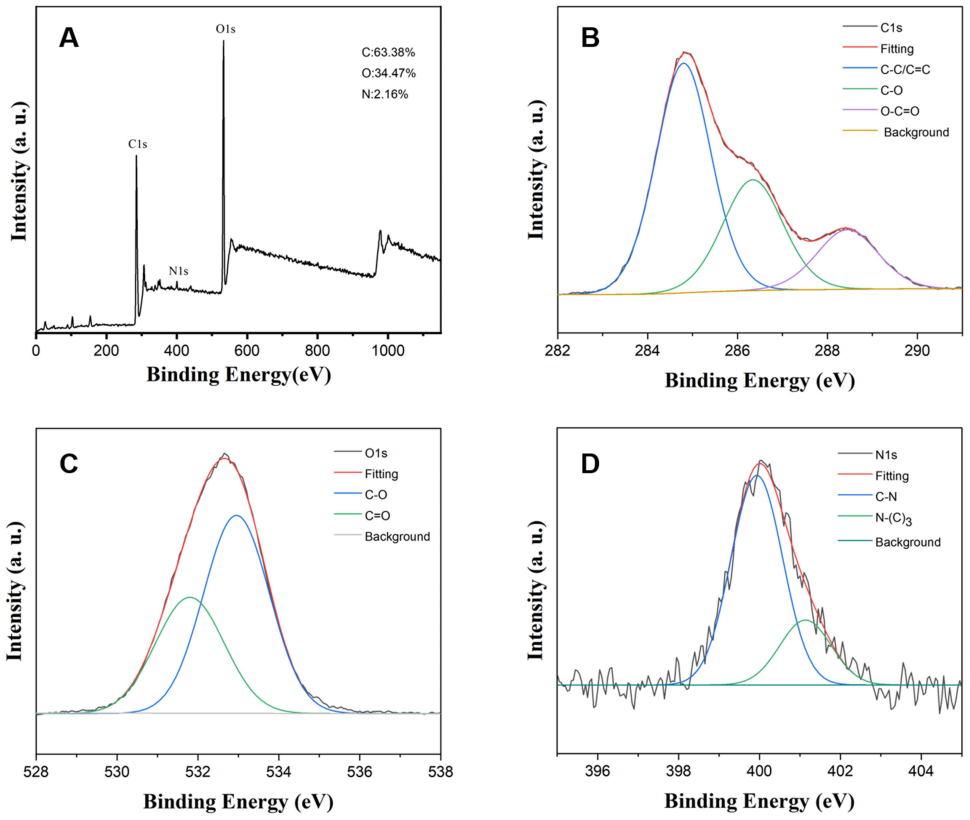

Figure 3 The XPS of MC-CDs. (**A**) Full-survey XPS data. (**B**) The high-resolution C1s spectrum. (**C**) The high-resolution O1s spectrum. (**D**) The high-resolution N1s spectrum.

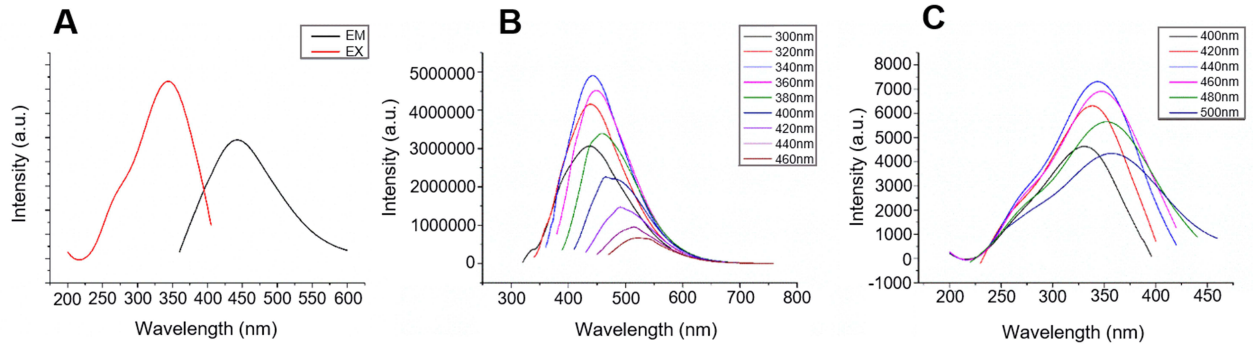

Figure 4 Luminescence properties of MC-CDs. (**A**) Emission and excitation wavelength fluorescence spectra. (**B**) Excitation spectra of the MC-CDs at emission wavelengths. (**C**) Emission spectra of the MC-CDs at different excitation wavelengths.

Pharmacokinetic Evaluation

Taking the square of the MA peak area as the abscissa, the linear equation was y = 4611.325x+13,765.59393 (r = 0.9589). The recovery rate of this method was more than 80%, the matrix effect was greater than 82%, the accuracy was between 111%-132%, the intraday precision was 4.42%, the intraday precision was 5.25%, and the stability was approximately 4.92%, indicating that the results obtained by this method were stable and reliable. The mean MA concentration-time curve is shown in Figure 7, and the main pharmacokinetic parameters are summarized in Table 1. Significantly different pharmacokinetic behaviors were observed between the MA control and MA-MC-CDs. The concentration of MA in rats treated with different concentrations of MA-MC-CDs was much higher than that of the

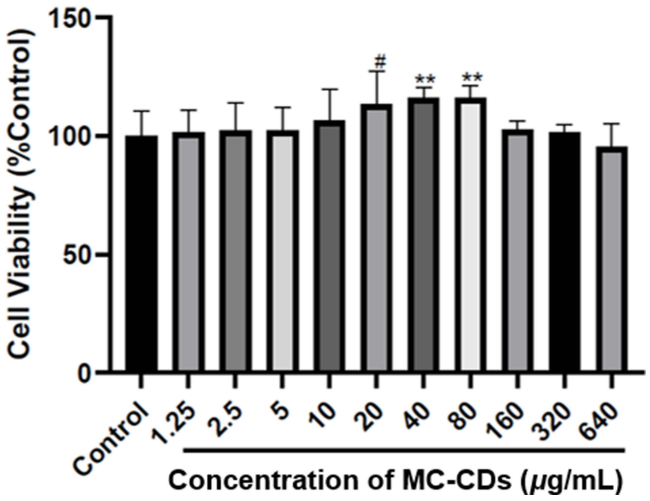

Figure 5 Cytotoxicity in HT-22 cells. All data are presented as the mean ± SD. #P < 0.05, **P < 0.01 between two groups.

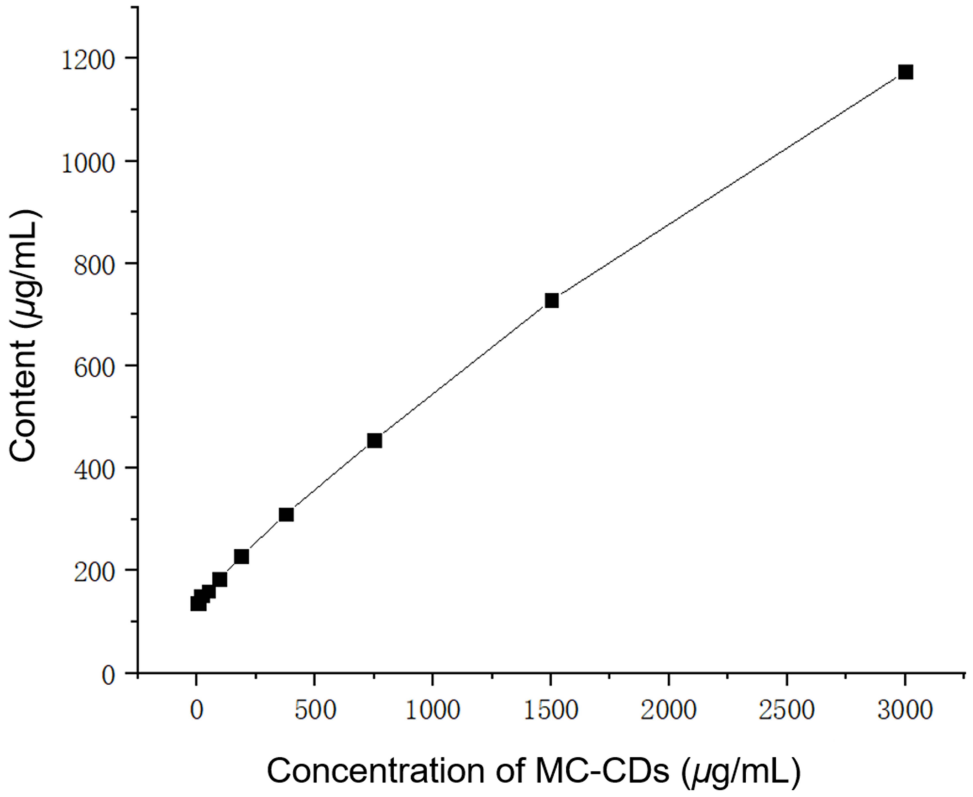

Figure 6 Concentration profiles of MA in the aqueous MC-CDs solutions.

MA control before 2.5 h, and the concentration of MA from MA-MC-CDs was lower than that of the MA control after 2.5 h, indicating that MA was rapidly absorbed and released into the bloodstream with the help of the MC-CDs.

The peak concentration C_{max} value of the MA from MA control and MA-MC-CDs in rats was 201.28 ± 31.38 ng/L and 323.98 ± 82.21 ng/L, respectively. h, respectively, compared T_{max} those of the control and MA-MC-CDs in rats was 4.00 ± 1.42 h and 0.25 ± 0.76 h, respectively. The $t_{1/2}$ value of the MA from MA control and MA treated with MC-CDs in rats was 3.27 ± 2.18 h and 7.22 ± 2.47 h, respectively. The CL/F value of the MA from MA control and MA treated with MC-CDs in rats was 11,144.46 ± 4039.27 L/h/kg and 14,490.30 ± 3335.50 L/h/kg, respectively. The AUC_{0-t} value

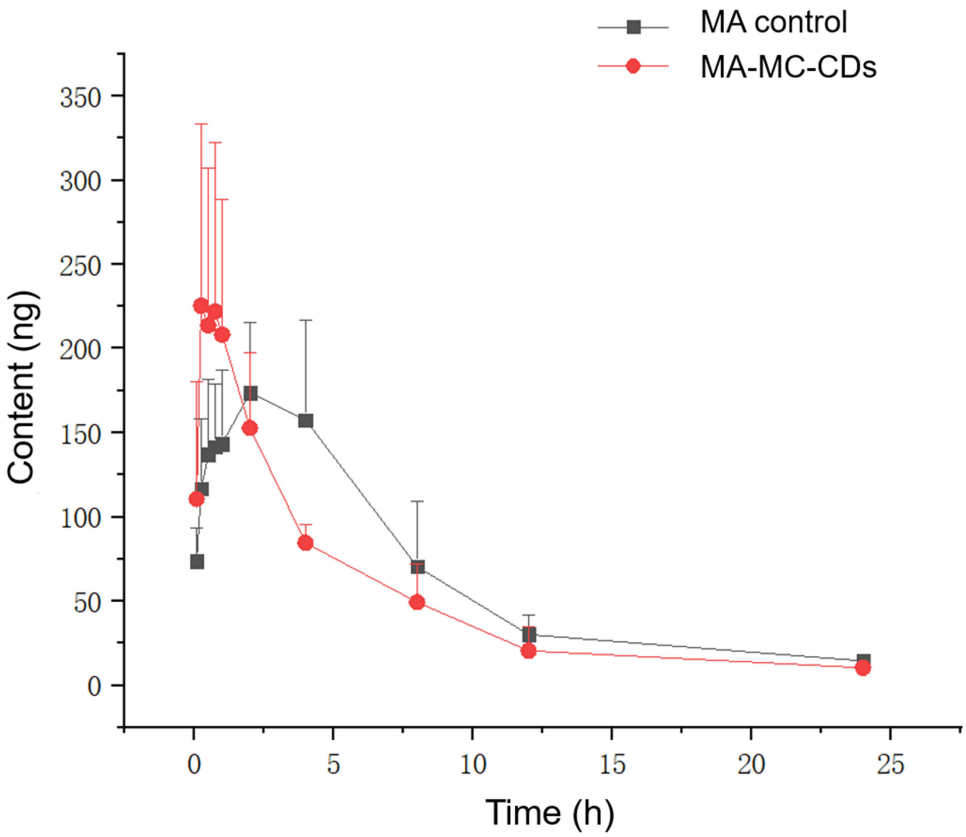

Figure 7 Effects of MC-CDs on the blood concentration-time curve of MA.

of the MA from MA control and MA treated with MC-CDs in rats was 1523.45 ± 2638.01 ng/L·h and 1249.81 ± 186.09 ng/L·h, respectively. In addition, the MRT value of MA from MA-MC-CDs was greater than that of the MA control. Collectively, these data revealed that MC-CDs effectively affected the pharmacokinetic parameters of MA in rats.

Discussion

MC-CDs have loose texture and good water solubility at 1–5 nm, and it can be found that when the concentration of MC-CDs exceeds 100 μg/mL, the solubility of MA in water increases significantly with the increase of MC-CDs concentration.

In a preliminary experiment on rat pharmacokinetics, methanol, acetonitrile, and acetonitrile-glacial acetic acid-precipitated protein were also investigated, and it was found that the recovery rate of plasma treated with acetonitrile-glacial acetic acid was high, in line with the requirements. After reviewing the literature, it was found that when the concentration of acetonitrile exceeded 1000 ng/mL, there was ion suppression, resulting in low extraction recovery.[53]

Table 1 Pharmacokinetic Parameters of MA in Rats After Oral Administration of MA Control and MA-MC-CDs

Parameter	Unit	MA	MA-MC-CDs
C_{max}	ng/L	201.28 ± 31.38	323.98 ± 82.21
T_{max}	h	4.00 ± 1.42	0.25 ± 0.76
$t_{1/2}$	h	3.27 ± 2.18	7.22 ± 2.47
CL/F	L/h/kg	11,144.46 ± 4039.27	14,490.30 ± 3335.50
AUC_{0-t}	ng/L·h	1523.45 ± 2638.01	1249.81 ± 186.09
MRT_{0-t}	h	5.23 ± 0.60	5.96 ± 1.55

Due to the poor oral absorption of MA, the maximum concentration was 200 ng, so the detection method of UPLC-MS /MS was established. This method has short analysis time, high sensitivity, and good detection results for low-content components.

It can be seen from the literature that the C_{max} of MA is low, and the T_{max} after oral administration is about 267.49 ± 108.29 min, which is basically consistent with the results of this experiment.[54] The addition of MC-CDs can increase the content of MA in vivo, shorten the time to reach the maximum concentration, extend the half-life of MA, and increase the apparent volume. To promote the absorption of drugs in the body, the onset time should be shortened to maintain efficacy so that the drugs can enter organs and tissues from the blood vessels faster.[55]

Our study shows that the novel carbon dots derived from natural *Moutan Cortex* significantly improve the solubility and bioavailability of mangiferin, which indicating its potential as a drug delivery system to improve the biopharmaceutical properties of other insoluble drugs. Several researches also supported the enormous promise of nanoparticles derived from natural sources.[56–58] In particular, the carbon dots from natural sources as the only source would possess infinite opportunities in the pharmaceutical and bio-technological industry.

Conclusion

Moutan Cortex-derived novel CDs exhibited excellent performance in improving the solubility and bioavailability of MA. The results of the CCK-8 assay showed that the MC-CDs have low cytotoxicity and can be used in various organisms. Because it contains -OH and -NH, it can form intramolecular hydrogen bonds with the phenolic hydroxyl groups of MA to increase the solubility of MA, and the formation of complex junction stability increases the content of MA in vivo, and the peak time is advanced from 4 h to 0.25 h. This study not only opens new possibilities for the future clinical application of MA but also provides evidence for the development of green biological carbon dots as a drug delivery system to improve the biopharmaceutical properties of insoluble drugs.

Data Sharing Statement

The data supporting the findings of this study are available upon request from the corresponding author.

Ethics Approval

All experiments and procedures were performed according to the animal study protocol approved by the Animal Care Ethics Committee of Anhui University of Chinese Medicine. All experiments were performed in accordance with the Guidelines for Ethical Conduct in the Care and Use of Animals.

Acknowledgments

We acknowledge the support from the Department of Material Science and Information Technology, Anhui University.

Funding

This work was supported by the Natural Science Foundation of Anhui Province (2308085MH304), the National Natural Science Foundation of China (82304324), the Research Foundation of Education Bureau of Anhui Province (2022AH050472, 2023AH040101), and the High-level Talents Support Project of Anhui University of Chinese Medicine (2022rczd011).

Disclosure

The authors declare that they have no conflicts of interest in this work.

References

1. Jyotshna Khare P, Shanker K, Shanker K. Mangiferin: a review of sources and interventions for biological activities. *Biofactors*. 2016;42 (5):504–514. doi:10.1002/biof.1308
2. Karim AA, Azlan A. Fruit pod extracts as a source of nutraceuticals and pharmaceuticals. *Molecules*. 2012;17(10):11931–11946. doi:10.3390/molecules171011931

3. Jiang T, Han F, Gao G, Liu M. Mangiferin exert cardioprotective and anti-Apoptotic effects in heart failure-induced rats. *Life Sci*. 2020;249:117476. doi:10.1016/j.lfs.2020.117476
4. Matkowski A, Kus P, Goralska E, Wozniak D. Mangiferin-A bioactive xanthonoid, not only from Mango and not just antioxidant. *MRMC*. 2013;13:439–455.
5. Khurana RK, Kaur R, Lohan S, Singh KK, Singh B. Mangiferin: a Promising anticancer bioactive. *Pharm Pat Anal*. 2016;5(3):169–181. doi:10.4155/ppa-2016-0003
6. Ichiki H, Miura T, Kubo M, et al. New antidiabetic compounds, mangiferin and its glucoside. *Biol Pharm Bull*. 1998;21(12):1389–1390. doi:10.1248/bpb.21.1389
7. Garrido G, Gonzalez D. In vivo and in vitro anti-inflammatory activity of Mangifera indica L. extract (VIMANG). *Pharmacol Res*. 2004;50 (2):143–149. doi:10.1016/j.phrs.2003.12.003
8. Li XJ, Du ZC, Huang Y, et al. Synthesis and hypoglycemic activity of esterified-derivatives of mangiferin. *Chin J Nat Med*. 2013;11(3):296–301. doi:10.3724/SP.J.1009.2013.00296
9. Yuan YF, Deng JG. Preparation of mangiferin monosodium salt. *Chin J Hosp Pharm*. 2008;28:281.
10. Liao HL, Qiu-Ye WU, Hong-Gang HU, Zang ZH, Song L, Yang Q. Structure modification of mangiferin. *West China J Pharm Sci*. 2008;23:385–387.
11. Pleguezuelos-Villa M, Nácher A, Hernández MJ, Ofelia Vila Buso MA, Ruiz Sauri A, Díez-Sales O. Mangiferin nanoemulsions in treatment of inflammatory disorders and skin regeneration. *Int J Pharm*. 2019;564:299–307. doi:10.1016/j.ijpharm.2019.04.056
12. Xuan XY, Wang YJ, Tian H, Pi JX, Zhang WL. Study on prescription of self-microemulsifying drug delivery system of mangiferin phospholipid complex. *J Chin. Med Mater*. 2012;35:1508–1511.
13. Bhattacharyya S, Ahmmed SM, Saha BP, Mukherjee PK. Soya phospholipid complex of mangiferin enhances its hepatoprotectivity by improving its bioavailability and pharmacokinetics. *J. Sci. Food Agric*. 2014;94(7):1380–1388. doi:10.1002/jsfa.6422
14. Zhou H, Han YM, Zheng YM, et al. Preparative procedure of inclusion compound of mangiferin-HP-*β*-CD. *J Chongqing Inst Technol*. 2009;9:11.
15. Mao X, Liu L, Cheng L, et al. Adhesive nanoparticles with inflammation regulation for promoting skin flap regeneration. *J. Control. Release*. 2019;297:91–101. doi:10.1016/j.jconrel.2019.01.031
16. Liu R, Liu Z, Zhang C, Zhang B. Nanostructured lipid carriers as novel ophthalmic delivery system for mangiferin: improving in vivo ocular bioavailability. *J Pharm Sci*. 2012;101(10):3833–3844. doi:10.1002/jps.23251
17. Cheng H, Zhao Y, Wang Y, et al. The potential of novel synthesized Carbon Dots derived resveratrol using one-pot green method in accelerating in vivo Wound Healing. *Int J Nanomed*. 2023;18:6813–6828. doi:10.2147/IJN.S434071
18. Chen HB, Khemtong C, Yang XL, Chang X, Gao J. Nanonization strategies for poorly water soluble drugs [J]. *Drug Discov Today*. 2011;16(7–8):354–360. doi:10.1016/j.drudis.2010.02.009
19. Magdy G, Aboelkassim E, El-Domany RA, Belal F. Ultrafast one-pot microwave-assisted green synthesis of silver nanoparticles from Piper longum fruit extract as a sensitive fluorescent nanoprobe for carbamazepine and risperidone in dosage forms and human plasma. *Microchem J*. 2024;197:109755. doi:10.1016/j.microc.2023.109755
20. Magdy G, Aboelkassim E, El-Domany RA, Belal F. Green synthesis, characterization, and antimicrobial applications of silver nanoparticles as fluorescent nanoprobes for the spectrofluorimetric determination of ornidazole and miconazole. *Sci Rep*. 2022;12(1):21395. doi:10.1038/s41598-022-25830-x
21. El Hamd MA, El-Maghrabey M, Almawash S, El-Shaheny R, Magdy G. Self-ratiometric fluorescence approach based on plant extract-assisted synthesized silver nanoparticles for the determination of vanillin. *Mikrochim Acta*. 2023;191(1):16. doi:10.1007/s00604-023-06093-3
22. Magdy G, Aboelkassim E, Abd Elhaleem SM, Belal F. A comprehensive review on silver nanoparticles: synthesis approaches, characterization techniques, and recent pharmaceutical, environmental, and antimicrobial applications. *Microchem J*. 2024;196:109615. doi:10.1016/j.microc.2023.109615
23. Huang X, Zafar A, Ahmad K, et al. Biological synthesis of bimetallic hybrid nanocomposite: a remarkable photocatalyst, adsorption/desorption and antimicrobial agent. *Appl Surf Sci Adv*. 2023;17:100446. doi:10.1016/j.apsadv.2023.100446
24. Saif MS, Hasan M, Zafar A, et al. Advancing nanoscale science: synthesis and bioprinting of zeolitic imidazole framework-8 for enhanced anti-infectious therapeutic efficacies. *Biomedicines*. 2023;11(10):2832. doi:10.3390/biomedicines11102832
25. Yu H, Saif MS, Hasan M, et al. Designing a silymarin nanopercolating system using CME@ZIF-8: an approach to hepatic injuries. *ACS Omega*. 2023;8(50):48535–48548. doi:10.1021/acsomega.3c08494
26. Magdy G, Elmansi H, Belal F, El-Deen AK. Doped carbon dots as promising fluorescent nanosensors: synthesis, characterization, and recent applications. *Curr Pharm Des*. 2023;29(6):415–444. doi:10.2174/1381612829666221103124856
27. Magdy G, Abdel Hakiem AF, Belal F, Abdel-Megied AM. Green one-pot synthesis of nitrogen and sulfur co-doped carbon quantum dots as new fluorescent nanosensors for determination of salinomycin and maduramicin in food samples. *Food Chem*. 2021;343:128539. doi:10.1016/j.foodchem.2020.128539
28. Magdy G, Al-Enna AA, Belal F, El-Domany RA, Abdel-Megied AM. Application of sulfur and nitrogen doped carbon quantum dots as sensitive fluorescent nanosensors for the determination of saxagliptin and gliclazide. *R Soc Open Sci*. 2022;9(6):220285. doi:10.1098/rsos.220285
29. Alossaimi MA, Elmansi H, Alajaji M, Altharawi A, Altamimi ASA, Magdy G. A novel quantum dots-based fluorescent sensor for determination of the anticancer dacomitinib: application to dosage forms. *Molecules*. 2023;28(5):2351. doi:10.3390/molecules28052351
30. Alossaimi MA, Altamimi ASA, Elmansi H, Magdy G. Green synthesized nitrogen-doped carbon quantum dots for the sensitive determination of larotrectinib in biological fluids and dosage forms: evaluation of method greenness and selectivity. *Spectrochim Acta A Mol Biomol Spectrosc*. 2023;300:122914. doi:10.1016/j.saa.2023.122914
31. El Hamd MA, El-Maghrabey M, Almawash S, Radwan AS, El-Shaheny R, Magdy G. Citrus/urea nitrogen-doped carbon quantum dots as nanosensors for vanillin determination in infant formula and food products via factorial experimental design fluorimetry and smartphone. *Luminescence*. 2024;39(2):e4643. doi:10.1002/bio.4643
32. Magdy G, Ebrahim S, Belal F, El-Domany RA, Abdel-Megied AM. Sulfur and nitrogen co-doped carbon quantum dots as fluorescent probes for the determination of some pharmaceutically-important nitro compounds. *Sci Rep*. 2023;13(1):5502. doi:10.1038/s41598-023-32494-8

33. Magdy G, Said N, El-Domany RA, Belal F. Nitrogen and sulfur-doped carbon quantum dots as fluorescent nanoprobes for spectrofluorimetric determination of olanzapine and diazepam in biological fluids and dosage forms: application to content uniformity testing. *BMC Chem*. 2022;16(1):98. doi:10.1186/s13065-022-00894-y
34. Li S, Li L, Tu HY. The development of carbon dots: from the perspective of materials chemistry. *Mater Today*. 2021;51:188–207. doi:10.1016/j.mattod.2021.07.028
35. Ali H, Ghosh S, Jana NR. Fluorescent carbon dots as intracellular imaging probes. *Wiley Interdiscip Rev Nanomed Nanobiotechnol*. 2020;12(4):e1617. doi:10.1002/wnan.1617
36. Liuye SQ, Cui SQ, Lu MM, Pu SZ. Construction of a photo controlled fluorescent switching with diarylethene modified carbon dots. *Nanotechnology*. 2022;33(40):405705. doi:10.1088/1361-6528/ac48ba
37. Ross S, Wu RS, Wei SC, Ross GM, Chang HT. The analytical and biomedical applications of carbon dots and their future theranostic potential: a review. *J Food Drug Anal*. 2020;28(4):677–695. doi:10.38212/2224-6614.1154
38. Chimento A, De Amicis F, Sirianni R, et al. Progress to improve oral bioavailability and beneficial effects of resveratrol. *Int J Mol Sci*. 2019;20(6):1381. doi:10.3390/ijms20061381
39. Zeng M, Wang Y, Liu M, et al. Potential efficacy of herbal medicine-derived Carbon Dots in the treatment of diseases: from mechanism to clinic. *Int J Nanomed*. 2023;18:6503–6525. doi:10.2147/IJN.S431061
40. Koutsogiannis P, Thomou E, Stamatis H, Gournis D, Rudolf P. Advances in fluorescent carbon dots for biomedical applications. *Adv Phy*. 2020;2:5.
41. Luo J, Kong H, Zhang M. Novel Carbon dots derived from Radix Pueraria Carbonisata Significantly Improve the Solubility and Bioavailability of Baicalin. *J Biomed Nanotechnol*. 2019;15(1):151–161. doi:10.1166/jbn.2019.2675
42. Tseng YT, Hsu YY, Shih YT, Lo YC. Paeonol attenuates microglia-mediated inflammation and oxidative stress-induced neurotoxicity in rat primary microglia and cortical neurons. *Shock*. 2012;37(3):312–318. doi:10.1097/SHK.0b013e31823fe939
43. Koo YK, Kim JM, Koo JY, Kang SS, Bae K, Kim YS. Platelet anti-aggregatory and blood anti-coagulant effects of compounds isolated from *Paeonia lactiflora* and *Paeonia suffruticosa*. *Pharmazie*. 2010;65(8):624–628.
44. Zhang L, Tao L, Shi TL, Zhang F, Sheng XB, Cao YZ. Paeonol inhibits B16F10 melanoma metastasis in vitro and in vivo via disrupting proinflammatory cytokines-mediated NF-κB and STAT3 pathways. *IUBMB Life*. 2015;67(10):778–788. doi:10.1002/iub.1435
45. Liu KYP, Hu SQ, Chan BCL, Wat ECL, Lau CBS, Hin KL. Anti-inflammatory and anti-allergic activities of pentaherb formula, moutan cortex (Danpi) and gallic acid. *Molecules*. 2013;18(3):2483–2500. doi:10.3390/molecules18032483
46. Ha DH, Trung TN, Hien TT, Dao TT, Yim N, Ngoc TM. Selected compounds derived from Moutan Cortex stimulated glucose uptake and glycogen synthesis via AMPK activation in human HepG2 cells. *J Ethnopharmacol*. 2010;131(2):417–424. doi:10.1016/j.jep.2010.07.010
47. Li Y, Liu X, Zheng Y, et al. Ultrasmall cortex moutan nanoclusters for the therapy of pneumonia and colitis. *Adv Healthc Mater*. 2023;12(18):e2300402. doi:10.1002/adhm.202300402
48. Yuan Y, Li B, Kuang Y, et al. The fiber metabolite butyrate reduces gp130 by targeting TRAF5 in colorectal cancer cells. *Cancer Cell Int*. 2020;20(1):212. doi:10.1186/s12935-020-01305-9
49. Pharmacopoeia Committee. *Pharmacopoeia of the People's Republic of China*. Beijing: Chinese Medical Science and Technology Press; 2020:240–241.
50. John BK, Abraham T, Mathew B. A review on characterization techniques for carbon quantum dots and their applications in agrochemical residue detection. *J Fluoresc*. 2022;32(2):449–471. doi:10.1007/s10895-021-02852-8
51. Stan L, Volf I, Stan CS, et al. Intense blue photo emissive carbon dots prepared through pyrolytic processing of ligno-cellulosic wastes. *Nanomaterials*. 2022;13(1):131. doi:10.3390/nano13010131
52. Karami MH, Pourmadadi M, Abdouss M, et al. Novel chitosan/γ-alumina/carbon quantum dot hydrogel nanocarrier for targeted drug delivery. *Int J Biol Macromol*. 2023;251:126280. doi:10.1016/j.ijbiomac.2023.126280
53. Han DD, Chen CJ, Zhang C, Zhang Y, Tang X. Determination of mangiferin in rat plasma by liquid–liquid extraction with UPLC–MS/MS. *J Pharmaceut Biomed*. 2010;51(1):260–263. doi:10.1016/j.jpba.2009.07.021
54. Sun YG, Du YF, Yang K. A comparative study on the pharmacokinetics of a traditional Chinese herbal preparation with the single herb extracts in rats by LC–MS/MS method. *J Pharmaceut Biomed*. 2013;81:34–43. doi:10.1016/j.jpba.2013.03.022
55. Lv F, Hasan M, Dang H, et al. Optimized luteolin loaded solid lipid nanoparticle under stress condition for enhanced bioavailability in rat plasma. *J Pharmaceut Biomed*. 2016;16:9443–9449.
56. Hasan M, Iqbal J, Awan U, et al. LX loaded nanoliposomes synthesis, characterization and cellular uptake studies in H_2O_2 stressed SH-SY5Y cells. *J Nanosci Nanotechnol*. 2014;14(6):4066–4071. doi:10.1166/jnn.2014.8201
57. Murtaza H, Ayesha Z, Maryam Y, et al. Synthesis of loureirin B-loaded nanoliposomes for pharmacokinetics in rat plasma. *ACS Omega*. 2019;4(4):6914–6922. doi:10.1021/acsomega.9b00119
58. Dang H, Meng MHW, Zhao H, et al. Luteolin-loaded solid lipid nanoparticles synthesis, characterization, & improvement of bioavailability, pharmacokinetics in vitro and vivo studies. *J Nanopart Res*. 2014;16(4):2347. doi:10.1007/s11051-014-2347-9